tvst

Article

Malondialdehyde-Modified Photoreceptor Outer Segments Promote Choroidal Neovascularization in Mice

Yuhong Chen[1,2,*], Xinyue Zhu[1,2,*], Fuxiang Ye[1,2,*], Hong Wang[1,2], Xiaoling Wan[1–3], Ting Zhang[1–3], Yuwei Wang[1,2], Yimin Wang[1,2], Xiaohuan Zhao[1,2], Xinyue Bai[1,2], Yushu Xiao[1,2], and Xiaodong Sun[1–4]

[1] Department of Ophthalmology, Shanghai General Hospital, Shanghai Jiao Tong University, School of Medicine, Shanghai, China
[2] National Clinical Research Center for Eye Diseases, Shanghai, China
[3] Shanghai Key Laboratory of Fundus Diseases, Shanghai, China
[4] Shanghai Engineering Center for Visual Science and Photomedicine, Shanghai, China

Correspondence: Fuxiang Ye and Xiaodong Sun, Department of Ophthalmology, Shanghai General Hospital, Shanghai Jiao Tong University School of Medicine, 100 Haining Rd, Shanghai 200080, China. e-mail: yefux@sjtu.edu.cn and xdsun@sjtu.edu.cn

Received: June 24, 2021
Accepted: December 10, 2021
Published: January 11, 2022

Keywords: age-related macular degeneration; malondialdehyde; retinal pigment epithelium; choroidal neovascularization; mouse model

Citation: Chen Y, Zhu X, Ye F, Wang H, Wan X, Zhang T, Wang Y, Wang Y, Zhao X, Bai X, Xiao Y, Sun X. Malondialdehyde-modified photoreceptor outer segments promote choroidal neovascularization in mice. Transl Vis Sci Technol. 2022;11(1):12, https://doi.org/10.1167/tvst.11.1.12

Purpose: This study aimed to establish a novel choroidal neovascularization (CNV) mouse model through subretinally injecting malondialdehyde (MDA)-modified photoreceptor outer segments (POS), which was more consistent with the pathogenesis of wet age-related macular degeneration (AMD).

Methods: MDA-modified POS were subretinally injected in C57BL/6J mice. Four weeks later, to assess the volume of CNV and the morphology of retinal pigment epithelium (RPE), isolectin B4 and zonula occludens-1 antibody were used for immunostaining. Fundus fluorescent angiography and optical coherence tomography imaging were used to describe the morphologic features of CNV. Transepithelial resistance was measured on polarized ARPE-19 cells. Vascular endothelial growth factor levels in the cell culture medium were detected by enzyme-linked immunosorbent assay. The protein and messenger RNA expression levels of autophagy markers were measured using Western blot and quantitative polymerase chain reaction.

Results: CNV and RPE atrophy were successfully induced in the mouse model. MDA-modified POS also significantly increased the expression of vascular endothelial growth factor and disrupted cell junctions in RPE cells. In addition, MDA-modified POS induced autophagy–lysosomal impairment in RPE cells.

Conclusions: Subretinal injection of MDA-modified POS may generate a feasible CNV model that simulates the AMD pathological process.

Translational Relevance: This study expands the understanding of the role of MDA in AMD pathogenesis, which provides a potential therapeutic target of AMD.

Introduction

Age-related macular degeneration (AMD) is a disease that causes progressive loss of central vision and is one of the leading causes of irreversible blindness worldwide.[1] The late-stage AMD manifests as geographic atrophy (dry AMD) and neovascular (wet) AMD. The pathophysiological mechanisms leading to AMD are not fully understood, but genetic predisposition and environmental factors, including oxidative stress and smoking, are believed to play key roles.

Lipids are the major target for reactive oxygen species.[2] Polyunsaturated fatty acids (PUFAs) can be readily oxidized to produce lipid hydroperoxides and several aldehydes.[3] Peroxides and metabolites generated from the PUFAs peroxidation are crucial factors in the pathogenesis of RPE damage.[4] Malondialdehyde (MDA), the principal end-product of PUFA peroxidation, is regarded as a marker of oxidative stress.[5,6]

A number of studies found that serum MDA levels in patients with wet AMD were significantly higher compared with patients without AMD. Also, in eyes with wet AMD, there was a correlation between MDA level and choroidal neovascularization (CNV) lesion area.[7–9] Our previous study showed that linoleic acid, the most abundant dietary ω-6 PUFA, promoted CNV progression in mice with elevated MDA levels.[10]

AMD is widely known as a kind of lipofuscin-related retinal degeneration and related to retinal pigment epithelium (RPE) dysfunction. To avoid intracellular accumulation, the RPE transports nutrients and metabolites between the microvascular beds, which maintain the outer retina, and photoreceptor neurons and removes photoreceptor outer segments (POS) by receptor-mediated phagocytosis.[11–14] POS degradation disorders in senescent RPE cells play an essential role in the initiation of AMD, which causes drusen-like deposits. As a consequence of continuous POS digestion, among that of cells in other retinal regions, the lysosomal apparatus of RPE cells in the macular region bears the greatest load because it digests the most material. Impairment of the lysosomal degradative capacity of the RPE is assumed to play an essential role in the initiation of pathophysiological events, finally causing functional and morphological damage to the RPE, resulting in degeneration of the corresponding neurosensory retina.[15–17]

MDA is prone to react with proteins or nucleosides to form MDA–protein or MDA–DNA adducts, which are believed to induce alterations of biochemical properties and the accumulation of biomolecules in chronic diseases and aging.[18,19] Proteomic analysis of ocular lipofuscin granules revealed that various lipofuscin proteins are damaged by lipid peroxidation-derived modifications.[20,21] A prior study suggested that a variety of lipofuscin-associated proteins are damaged by the aberrant covalent modification of MDA. These damaged proteins are more resistant to proteolytic attack and act as protease inhibitors.[22] MDA-modified POS, as an experimental model of MDA adducts, were found to be phagocytosed by RPE cells, which consequently induced lysosomal dysfunction in consequence.[23,24] It is acknowledged that RPE cell tight junctions work well to prevent CNV. We speculate that MDA-modified POS, rather than unmodified POS, are pivotal pathogenic factors in AMD. However, little is known about the role of MDA-modified POS in an in vivo model. In the present study, we found that MDA-modified POS induced CNV and RPE damage in mice. We aimed to explore the potential pathological mechanism of AMD using this AMD-like mouse model to identify the possible target of AMD and to determine a potential preventive treatment for AMD.

Methods

Preparation of the MDA Solution

MDA was prepared as described previously.[25–27] Briefly, malonaldehyde bis-(dimethyl acetal), also known as 1,1,3,3-tetramethoxypropane (Sigma-Aldrich, St. Louis, MO), was treated with HCl (pH, 1.0) for 60 min in a water bath at 50°C. The solution was further diluted to a concentration of 500 µM with phosphate-buffered saline (PBS), and the pH was then adjusted to 7.4 using a NaOH solution.

Porcine POS Isolation and MDA Modification

Porcine eyes were purchased from a local abattoir. Porcine POS were immediately isolated following a published procedure.[28] MDA-modified POS were prepared using a previously described method.[23,24] In brief, POS were centrifuged at 5000 rpm for 7 min and then resuspended in a 500 µM MDA solution or PBS. The mixtures were incubated overnight at 4°C on a shaker to synthesize MDA adducts. The POS were then centrifuged at 5000 rpm for 7 min three times again, after which the POS were washed with PBS to remove unbound MDA.

ARPE-19 Cell Culture

ARPE-19 cells, a human RPE cell line, were purchased from the American Type Culture Collection (Rockville, MD). For regular (nonpolarized) culture, the cells were grown in Dulbecco's Modified Eagle's Medium premixed with Ham's F-12 (1:1 ratio; Sigma-Aldrich) and supplemented with 10% (v/v) fetal bovine serum (FBS, Thermo Fisher Scientific, Waltham, MA) and the antibiotics streptomycin and penicillin G (Thermo Fisher Scientific) at 37°C in a humidified atmosphere of 5% (v/v) CO_2. When the cells were 80% confluent, they were treated with MDA-modified POS for 48 hours. In brief, after washing with PBS three times, MDA-modified POS were diluted to 600 µg/mL and 300 µg/mL with the culture medium and then plated on the wells. Wells with 600 µg/mL unmodified POS and medium alone were used as controls.

Polarized Cell Culture

Polarized ARPE-19 cell culture was performed as described previously.[29–32] In brief, ARPE-19 cells (approximately 1.65×10^5 cells/well) were seeded onto Transwell filters (12 mm internal diameter, 0.4 µm pore size; Corning, NY) precoated with

Matrigel (BD Biosciences, San Jose, CA). The cells were maintained for 8 weeks in a mixed medium consisting of α-modified Eagle's minimum essential medium, N1 supplement (N-6530; 5 mL/500 mL), nonessential amino acids (M-7145; 5 mL/500 mL), L-glutamine–penicillin–streptomycin (G-1146; 5 mL/500 mL), taurine (T-0625; 125 mg/500 mL), hydrocortisone (H-0396; 10 µg/500 mL), tri-iodothyronine (T-5516; 0.0065 µg/500 mL) (Sigma-Aldrich), and 1% (v/v) FBS. The polarized ARPE-19 cells were then treated with MDA-modified POS for 48 hours, as described elsewhere in this article. After washing with PBS three times, Transwell filters were fixed with 4% paraformaldehyde or 100% methanol.

Measurement of Transepithelial Resistance (TER)

The TER of the polarized RPE cells on the Transwell filters was measured with an Epithelial Voltohmmeter 2 (EVOM2; World Precision Instruments, Sarasota, FL) as described previously.[31,32] TER measurements were performed within 3 min after the removal of the cells from the incubator. The TER (Ω) was multiplied by the effective growth area (cm^2) to obtain TER–area products ($\Omega \cdot cm^2$), the final resistance per unit area. The TER in each well was measured at least three times, and the average value was calculated for analysis. The results are expressed as percent changes in TER relative to the control.

Enzyme-Linked Immunosorbent Assay

After treatment, the culture medium was collected. Vascular endothelial growth factor (VEGF) levels in the cell culture medium were measured using a human VEGF ELISA kit (R&D Systems, Minneapolis, MN) following the manufacturer's instructions. The plates were analyzed by measuring the absorbance at 450 nm with a reference at 570 nm using a plate reader (Infinite F50, Switzerland). Duplicate evaluations were performed for each sample.

Quantitative Real-Time Polymerase Chain Reaction

Total RNA was purified from cell lysates using an RNA Simple Total RNA kit (Tiangen, Beijing, China) according to the manufacturer's protocol. The RNA concentration and quality were assessed using a NanoDrop ND-2000 spectrophotometer (NanoDrop Technologies, Rockland, DE). The total RNA was reverse transcribed using Prime Script RT Master Mix (TaKaRa Bio, Shiga, Japan), starting with 2 µg of total RNA from each sample. Quantitative real-time polymerase chain reaction was performed using TB Green Premix Ex Taq (TaKaRa Bio, Shiga, Japan) and primers for human VEGF-A (F: 5′-CTACCTCACCATGCCAAGT-3′, R: 5′-GCAGTAGCTGCGCTGATAGA-3′) and 18S (F: 5′-TTCGTATTGCGCCGCTAGA-3′, R: 5′-CTTTCGCTCTGGTCCGTCTT-3′) RNA following the manufacturer's protocol.

Cell Viability Assay

The viability of ARPE-19 cells was measured using a Cell Counting Kit-8 assay (CCK-8, Yeasen, China) as described previously.[33] In brief, 5×10^3 ARPE-19 cells were seeded into 96-well plates and treated with 600 µg/mL MDA-modified or unmodified POS. After treatments, 10 µL/well CCK-8 reagent was added, and the plates were incubated for 2 more hours at 37°C and then analyzed by measuring the absorbance at 450 nm using a plate reader (Infinite F50). Duplicate evaluations were performed for each sample.

Measurement of MDA Levels

The levels of MDA in ARPE-19 cells were determined by using a detection kit from Solarbio (Beijing Solarbio Science & Technology Co., Ltd., Beijing, China) according to the manufacturer's instructions.

Animals

Male wild-type C57BL/6J mice were housed and bred in the Shanghai General Hospital animal facility. To examine the effects of MDA-modified POS on CNV growth, mice aged 6 to 8 weeks were subretinally injected with 2 µL of MDA-modified POS (50 mg/mL), unmodified POS (50 mg/mL), or PBS. Four weeks later, the eyes were enucleated and fixed with 4% (w/v) paraformaldehyde. All animal experiments were approved by the Shanghai General Hospital Animal Welfare and Ethics Committee.

Immunostaining

Eyecups were obtained from the fixed eyes by removing the anterior segments. To visualize the mouse CNV, the eyecups were incubated with 0.5% (w/v) fluorescein isothiocyanate-conjugated isolectin B4 (iB4; Sigma-Aldrich). To visualize the structure of the polarized ARPE-19 cells and mouse RPE, zonula occludens-1 (ZO-1) staining was performed in a manner similar to that described previously.[34,35]

In brief, the Transwell filters and the eyecups were stained with rabbit antibody against ZO-1 (Thermo Fisher Scientific), and visualized with Alexa-594 (Invitrogen, Carlsbad, CA) and 4′,6-diamidino-2-phenylindole (Molecular Probes, Eugene, OR). Images were obtained using a confocal microscope (Leica, Wetzlar, Germany).

Western Blotting

ARPE-19 cells were harvested in lysis buffer after indicated treatments. The proteins were loaded onto SDS-PAGE gels for electrophoresis and then transferred onto PVDF membranes. The membranes were separately incubated with primary antibodies against Tubulin, LC3B, Beclin-1, and p62 (Cell Signaling Technology, Beverly, MA) at 4°C overnight, followed by incubation with corresponding secondary antibodies coupled with horseradish peroxidase (Proteintech, Shanghai, China) at room temperature for 1 hour. Images were obtained using an Amersham imager (Buckinghamshire, UK).

Fundus Fluorescent Angiography (FFA)

Four weeks after subretinal injection, anesthetization and pupil dilation was performed. We injected 2% fluorescein sodium (Fluorescite; Alcon, Tokyo, Japan) intraperitoneally. FFA images were acquired using a Micron IV Retinal Imaging Microscope (Phoenix Research Labs, CA).

Optical Coherence Tomography (OCT) Imaging

The in vivo retinal imaging in mice was captured by using the Phoenix mouse OCT2 system (Phoenix Research Labs, Pleasanton, CA) 4 weeks after subretinal injection. Mice were anesthetized and positioned on a custom cassette that allowed three-dimensional free rotation to align the mouse eye for imaging. The scans of the retina were acquired across the CNV in the MDA-POS group and the position equidistant from the optic nerve head in the control group.

Statistical Analyses

The results are expressed as the means ± standard errors of the mean (n = number of samples). Values from the control sample were defined as 100%, and the percent change relative to the control value was calculated for each sample. All statistical analyses were performed using version 4.0.2 of R statistical software (open-source software available at http://www.r-project.org/). The *t* test was used for comparisons between two groups. Comparisons among three or more groups were analyzed with the Kruskal–Wallis test; if significance was detected ($P < 0.05$), the post hoc Steel's test (for the comparison of multiple treatment groups with the control) or Steel–Dwass test (for all pairs multiple comparisons) was performed. Comparisons among categorical variables were statistically analyzed using the Fisher exact test. Differences were considered to be statistically significant at a *P* value of less than 0.05

Results

Subretinal Injection of MDA-Modified POS Induced Mouse CNV and RPE Atrophy

To confirm the effects of MDA-modified POS on the mice, we subretinally injected MDA-modified and unmodified POS into 10 mouse eyes. Fluorescein isothiocyanate-conjugated iB4 staining showed the presence of CNV in 7 of the 10 eyes injected with MDA-modified POS, but in only 4 of the 10 eyes injected with unmodified POS by comparison. No CNV was observed in the eyes injected with PBS as a control ($P = 0.00494$; Fig. 1A). Meanwhile, the CNV volume seemed to be larger in the eyes injected with MDA-modified POS (Figs. 1B-D). Unlike the control group (Fig. 1E), the MDA-modified POS-induced CNV showed hyperfluorescent spots in FFA images, suggesting the presence of leakage from vessels (Fig. 1F). In the OCT images, MDA-modified POS-induced CNV was observed as a highly reflective area that was covered by a dome-shaped, highly reflective layer corresponding with the RPE (Fig. 1H), rather than the intact and smooth RPE layer in the control group (Fig. 1G). To further elucidate the effect of MDA-modified POS on the RPE in vivo, ZO-1 (an RPE junction-related molecule)[36,37] staining was performed. The hexagonal RPE in the eyes injected with POS showed a collapsed morphology. MDA-modified POS likely disrupted the RPE to a greater extent and increased the CNV volume (Fig. 2). The results above indicate that the subretinal injection of MDA-modified POS induced more spontaneous CNV and worse RPE atrophy.

MDA-Modified POS Disrupted Cell Junctions, Affected Cell Viability, and Promoted MDA Levels in RPE Cells

Cultured polarized RPE cells act as a model that simulates the in vivo RPE monolayer. In this study,

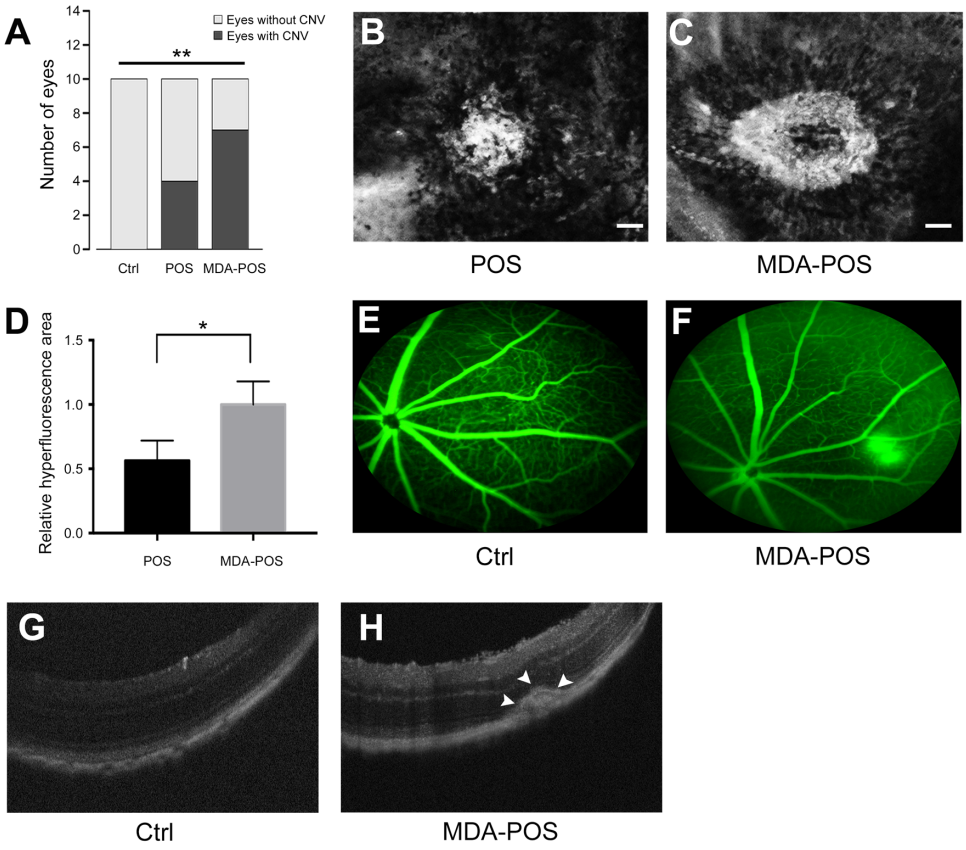

Figure 1. Subretinal injection of MDA-modified POS induced CNV in mice. (**A**) Fluorescein isothiocyanate-conjugated iB4 staining showed no CNV in any of the eyes in the control (PBS) group, but CNV was found in 4 of 10 eyes in the unmodified POS group, and 7 of 10 eyes in the MDA-modified POS group; the differences among the three groups were significant. (**B–D**) Representative flat-mounts of mouse choroids showed that the CNV volume in the unmodified POS group was smaller than that in the MDA-modified POS group (**E** and **F**) FFA at 4 weeks after subretinal injection. In the MDA-modified POS injection group, there was a hyperfluorescent spot. (**G** and **H**) Representative OCT scans at 4 weeks after subretinal injection. In the MDA-modified POS group, OCT images showed massive hyperreflectivity under the RPE layer, hyperreflective bands (*arrowheads*) at the border of the hyperreflective tissue, thinning outer nuclear layer (ONL), and disrupted photoreceptor layer. However, an intact and smooth RPE layer was observed in the control group. Scale bar, 50 µm. Ctrl, control. *$P < 0.05$ by *t* test, **$P < 0.01$ by Fisher's exact test.

we also assessed the effect of MDA-modified POS on polarized RPE cells. Polarized RPE cells were treated with POS for 48 hours, and cell junctions were visualized by ZO-1 staining. The disruption of RPE cell junctions was observed after POS treatment, and this disruption was more severe with the exposure of MDA modification (Fig. 3A). A high TER is characteristic of polarized cells. In this study, following the protocol of Sonoda et al,[31] we maintained polarized cells for 8 weeks and successfully cultured polarized cells with a TER higher than 200 $\Omega \cdot cm^2$. MDA-modified POS treatment significantly lowered the TER compared with that in the control group (-30.14%, Fig. 3B, $P = 0.00919$). These results revealed that POS, especially those modified with MDA, disrupted the morphology and function of RPE cell junctions. ARPE-19 cells under regular culture conditions were treated with unmodified or MDA-modified POS for 48 hours. Cell viability was measured by a CCK-8 assay and found to be suppressed significantly by POS treatment (unmodified $P = 0.00652$; MDA-modified $P = 0.0248$). However, the difference in viability between the two POS-treated groups was not significant ($P = 0.115$) (Fig. 3C), indicating that the modification of POS with MDA did not increase cytotoxicity to RPE cells. To exclude the possibility that RPE cells failed to ingest MDA-modified POS by phagocytosis, MDA levels were detected in cells and found a significant increase in the group treated with MDA-modified POS compared with the control group ($P < 0.0001$). However, the treatment with unmodified POS did not upregulate the MDA levels in ARPE-19 cells (Supplementary Fig. S1).

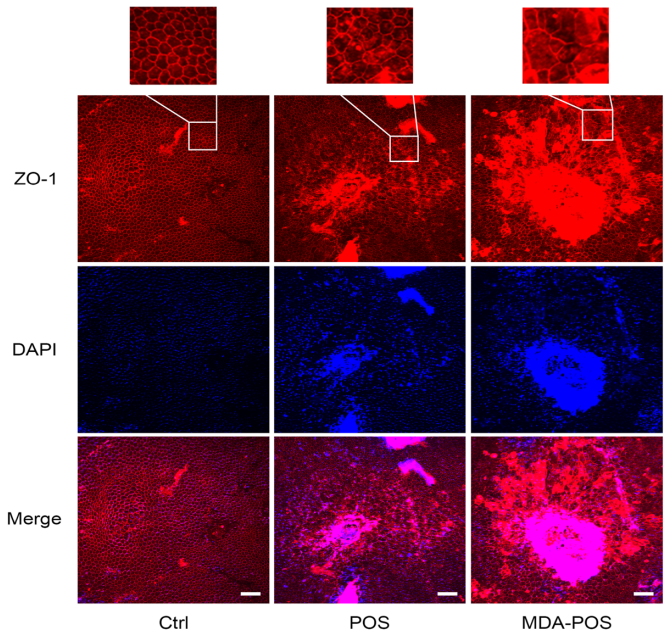

Figure 2. Subretinal injection of MDA-modified POS induced RPE disruption in mice. Four weeks after subretinal injection, mouse choroid flat-mounts were obtained. ZO-1 staining showed that compared with unmodified POS, MDA-modified POS disrupted RPE tight junctions to a greater extent and increased the CNV volume. Subretinal injection of PBS caused almost no damage to the RPE. The top row of pictures represent a higher magnification of initial pictures. Scale bar, 100 µm.

MDA-Modified POS Induced VEGF Expression in RPE Cells

Next, we explored the effects of MDA-modified POS on human RPE cells in vitro. After ARPE-19 cells had been treated with MDA-modified POS for 48 hours, VEGF messenger RNA expression in cells and the levels of VEGF secreted into the medium were measured. VEGF messenger RNA expression was significantly elevated by treatment with POS ($P = 0.0142$), although the difference was not significant between the unmodified and MDA-modified POS groups. ($P > 0.05$; Fig. 4A). Furthermore, the expression levels of VEGF in the medium of regular culture and polarized culture were also detected by enzyme e-linked immunosorbent assay. For both cell culture methods, MDA-modified POS significantly increased VEGF expression compared with that in the control groups treated with PBS (regular, $P = 0.0281$; polarized, $P = 0.00194$). VEGF was also significantly elevated in the groups treated with MDA-modified POS compared with those treated with unmodified POS (regular, $P = 0.0431$; polarized, $P = 0.0179$) (Fig. 4B, C). These results showed that POS could induce VEGF expression and that MDA modification enhanced this effect.

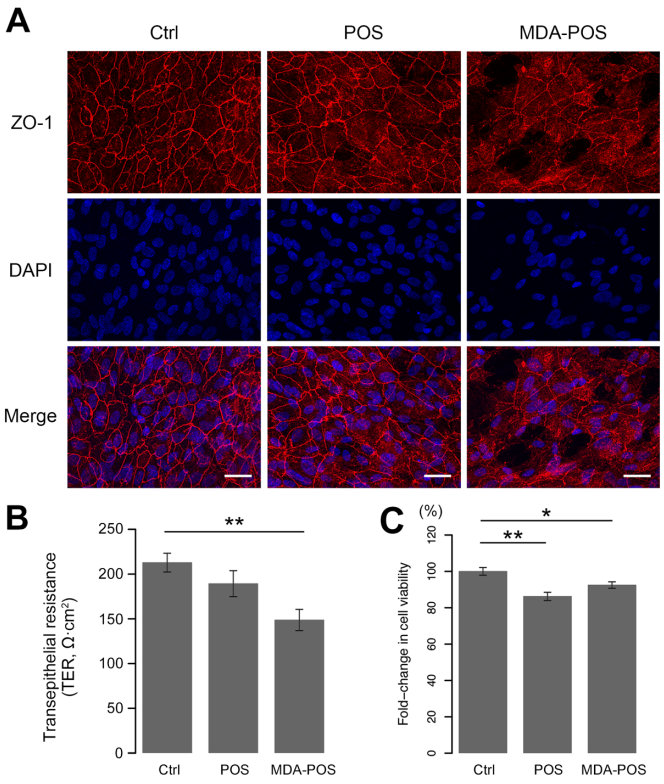

Figure 3. MDA-modified POS disrupted the cell junctions of RPE cells under polarized culture conditions. (**A**) ARPE-19 cells were cultured under polarized conditions for eight weeks. ZO-1 staining showed that POS disrupted RPE tight junctions, and MDA-modified POS caused greater destruction than unmodified POS. (**B**) MDA-modified POS treatment significantly decreased the TER compared with that in the control group, which indicated that the cell-cell junctions had been functionally damaged. (**C**) POS treatment suppressed the viability of RPE cells compared with that of the control cells, but MDA modification did not further inhibit cell viability. Data are shown as the mean ± standard error of the mean. *$P < 0.05$, **$P < 0.01$ by the Kruskal–Wallis test.

MDA-Modified POS Induced Autophagy–Lysosomal Impairment

In this study, to assess whether the autophagy–lysosomal pathway plays an essential role in the degradation of MDA-modified POS, we treated ARPE-19 cells with PBS or unmodified or MDA-modified POS. We indicated autophagy level by autophagy-associated proteins: Beclin1, p62, and LC3B. Beclin1 is a key protein in the process of autophagy lysozyme degradation, which is the mammalian homolog of Vps30p/Apg6p. p62, a protein that acts as a cargo receptor for the degradation of ubiquitinated proteins through autophagic or proteasomal pathways, possesses a short LC3 interaction region that facilitates direct interaction with LC3, and causes p62

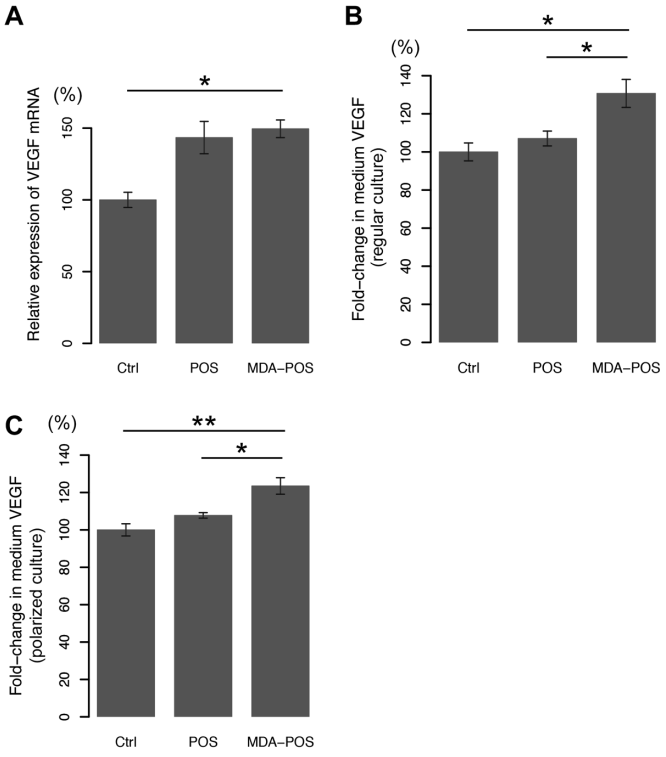

Figure 4. MDA-modified POS induced VEGF expression. (**A**) Real-time polymerase chain reaction showed that VEGF messenger RNA in ARPE-19 cells under regular culture conditions was elevated by POS treatment, while the difference in VEGF messenger RNA levels between the unmodified and MDA-modified POS groups was not significant. VEGF in RPE cells grown under not only regular culture conditions (**B**) but also polarized culture conditions (**C**) was also detected by enzyme e-linked immunosorbent assay. VEGF secreted into the medium was increased in both groups compared with the control group. Data are shown as the mean ± standard error of the mean. *$P < 0.05$, **$P < 0.01$ by the Kruskal–Wallis test with the post hoc Steel–Dwass test.

degradation by autophagy.[38–40] The presence of LC3 in autophagosomes and the conversion of LC3 to the lower migrating form, LC3-II, have been suggested as indicators of autophagy. Hence, the ratio of LC3-II/LC3-I is widely used as a marker of autophagy. ARPE-19 cells were treated with unmodified POS and different concentrations of MDA-modified POS (300 and 600 µg/mL); protein lysates were collected at different time points (0, 24, 48, and 72 hours). The autophagy levels were found dose- and time-dependently decreased (Supplementary Fig. S2). We then demonstrated that, after treatment for 48 hours, unmodified POS increased autophagy levels compared with those upon treatment with PBS. Whereas MDA-modified POS decreased the expression of autophagy markers Beclin1, the ratio of LC3-II/LC3-I and increased the levels of p62 in ARPE-19 cells (Fig. 5). These data suggested that the modification with MDA inhibited the autophagy-lysosomal pathway induced by POS treatment, which may be the mechanism by which RPE cells developed POS degradation disorders.

Discussion

RPE cells are polarized and maintain a barrier function,[31] allowing them to phagocytose POS phagosomes into acidified phagolysosomes, after which the enzymatic degradation of POS macromolecules occurs.[24,41] During aging and in degenerative retinal diseases, RPE dysfunction induces lipofuscinogenesis, the progressive accumulation of a complex polymer consisting of peroxidized lipids and protein residues.[42]

POS are highly susceptible to lipid peroxidation owing to the abundance of PUFAs in the disk membranes, extremely oxygen-rich environment, and constant light exposure.[43] Several electrophilic reactive aldehydes can be formed as secondary oxidation products during the decomposition of polyunsaturated lipid hydroperoxides. Examples of such aldehydes are α- and β- unsaturated aldehydes, for example, 4-hydroxy-2-nonenal, 4-hydroxy-2-hexenal, and MDA.[22]

Our previous study found MDA accumulation in AMD eyes; free MDA treatment induced the alternation of VEGF expression, disruption of cell junctions, and autophagy dysfunction in ARPE-19 cells.[10] As previously described, MDA-modified POS induced destruction of polarized RPE cells as well as lipofuscin-like deposits,[10,23,44] indicating that MDA-modified POS may contribute to the pathogenesis of AMD. MDA-modified POS have been found more resistant to proteolytic attack than unmodified POS because they induce more severe lysosomal dysfunction in RPE cells.[23,24] Others also found that MDA-modified POS affected the RPE through the autophagy–lysosomal pathway.[45] Our results showed that autophagy in RPE cells could be enhanced by POS, but this effect was inhibited by MDA modification. This finding can be explained by the revelation that MDA induced autophagy dysfunction in our previous study.[10]

In the widely used laser-induced CNV model, autophagic levels have been demonstrated increased on days 1, 3, and 5, whereas decreased to normal level after 1 week, which was similar to the change of VEGF protein expression.[46] Because oxidative stress has been reported as a decisive factor in dry-AMD, $NaIO_3$ and H_2O_2 as oxidative toxic agents were used as reproducible models of AMD. In these models, it is demonstrated that reactive oxygen species were involved in various cellular responses, including autophagic flux and mitochondrial dynamic.[47–49]

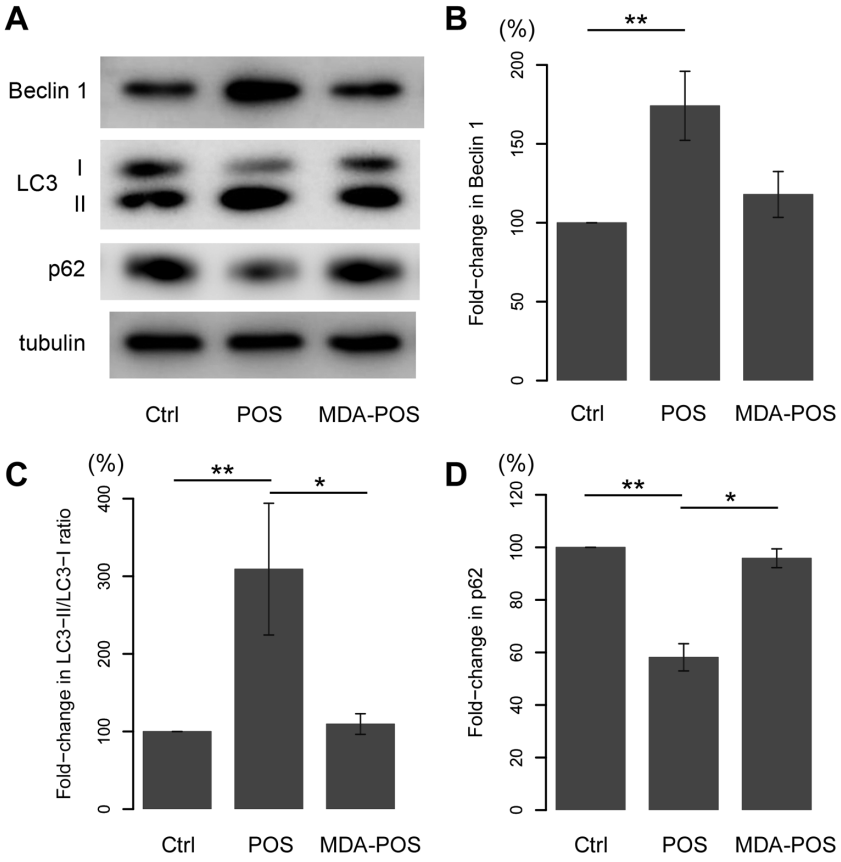

Figure 5. MDA-modified POS induced changes in autophagy-related proteins in RPE cells. (**A**) Western blot analysis showed that the protein levels of Beclin-1 and LC3-II/LC3-I ratio were significantly increased and that the protein level of p62 was decreased after unmodified POS treatment compared with those in the control group. However, after treatment with MDA-modified POS, the protein expression of autophagy markers followed opposite trends. (**B–D**) The expression level of each protein was normalized to the mean value in the control group. Data are shown as the mean ± standard error of the mean. *$P < 0.05$, **$P < 0.01$ by the Kruskal–Wallis test with post hoc Steel–Dwass test.

A higher autophagic level was suggested as a protective mechanism against oxidative stress. Dysfunction of autophagic pathways has been associated with neurodegenerative disease.[50,51] Much interest has focused on the role of autophagy in AMD.[52,53] Increasing evidence has indicated that cellular quality is associated with autophagy/mitophagy and mitochondrial dynamics in AMD. The autophagy disorder results in the accumulation of damaged proteins and dysfunctional organelles, especially the mitochondria, which generates enhanced reactive oxygen species levels that causes DNA damage, affects cell viability, and induces cell death.[54–57] Long-term and chronic oxidative stress can result in the premature aging of RPE cells, which is characterized by upregulated VEGF, 8-OHdG DNA damage lesions, mitochondrial dysfunction, and higher expression of senescence-associated secretory phenotype factors.[58–61]

The laser-induced CNV is generated by laser photocoagulation, which destroys Bruch's membrane. However, this model is an animal model of an acute injury that cannot simulate the chronic pathological process from dry to wet AMD. In this study, a mouse model was introduced for the first time to research MDA-modified POS. MDA-modified and unmodified POS were subretinally injected, and spontaneous CNV and an RPE atrophy-like pathology were found in the mice, providing evidence to suggest that excess POS at the RPE induce an AMD-like pathology and that MDA modification enhances this effect.

Our study has revealed the possible relationship between MDA-modified POS and AMD in vivo for the first time, providing a novel perspective for the study of AMD. The limitations of the study are as follows. (a) The microstructure of the RPE, which engulfed MDA-modified POS, was not observed. (b) Additionally, the precise mechanisms involved remain unclear. Further studies are needed to confirm the feasibility of animal CNV modeling induced by the subretinal injection of MDA-modified POS.

Conclusions

This study revealed that MDA-modified POS may be an agent to induce AMD-like pathology. Subretinal injection of MDA-modified POS may generate a feasible CNV model that simulates the AMD pathological process.

Acknowledgments

Supported by the National Natural Science Foundation of China (81700845 to FX. Ye), the National Natural Science Foundation of China, National Major Scientific and Technological Special Project for "Significant New Drugs Development" during the Thirtieth Five-year Plan Period, National Key R&D Program, Science and Technology Commission of Shanghai Municipality, Multi-center Clinical Research Project from Shanghai Jiao Tong University School of Medicine, Science and Technology Commission of Shanghai Municipality (81730026, 2019ZX09301113, 2017YFA0105301, 17411953000, DLY201813, 19495800700 to XD. Sun).

Disclosure: **Y. Chen**, None; **X. Zhu**, None; **F. Ye**, None; **H. Wang**, None; **X. Wan**, None; **T. Zhang**, None; **Y. Wang**, None; **Y. Wang**, None; **X. Zhao**, None; **X. Bai**, None; **Y. Xiao**, None; **X. Sun**, None

[*] YC, XZ and FY contributed equally to this work.

References

1. Mitchell P, Liew G, Gopinath B, et al. Age-related macular degeneration. *Lancet*. 2018;392(10153):1147–1159.
2. Niki E. Lipid peroxidation: physiological levels and dual biological effects. *Free Radic Biol Med*. 2009;47(5):469–484.
3. Uchida K. Aldehyde adducts generated during lipid peroxidation modification of proteins. *Free Radic Res*. 2015;49(7):896–904.
4. Njie-Mbye YF, Kulkarni-Chitnis M, Opere CA, et al. Lipid peroxidation: pathophysiological and pharmacological implications in the eye. *Front Physiol*. 2013;4:366.
5. Del Rio D, Stewart AJ, Pellegrini N. A review of recent studies on malondialdehyde as toxic molecule and biological marker of oxidative stress. *Nutr Metab Cardiovasc Dis*. 2005;15(4):316–328.
6. Yamauchi Y, Furutera A, Seki K, et al. Malondialdehyde generated from peroxidized linolenic acid causes protein modification in heat-stressed plants. *Plant Physiol Biochem*. 2008;46(8-9):786–793.
7. Ates O, Azizi S, Alp HH, et al. Decreased serum paraoxonase 1 activity and increased serum homocysteine and malondialdehyde levels in age-related macular degeneration. *Tohoku J Exp Med*. 2009;217(1):17–22.
8. Jia L, Dong Y, Yang H, et al. Serum superoxide dismutase and malondialdehyde levels in a group of Chinese patients with age-related macular degeneration. *Aging Clin Exp Res*. 2011;23(4):264–267.
9. Matsuura T, Takayama K, Kaneko H, et al. Nutritional supplementation inhibits the increase in serum malondialdehyde in patients with wet age-related macular degeneration. *Oxid Med Cell Longev*. 2017;2017:9548767.
10. Ye F, Kaneko H, Hayashi Y, et al. Malondialdehyde induces autophagy dysfunction and VEGF secretion in the retinal pigment epithelium in age-related macular degeneration. *Free Radic Biol Med*. 2016;94:121–134.
11. Anderson DH, Fisher SK, Steinberg RH. Mammalian cones: disc shedding, phagocytosis, and renewal. *Invest Ophthalmol Vis Sci*. 1978;17(2):117–133.
12. Gordon WC, Rodriguez de Turco EB, Bazan NG. Retinal pigment epithelial cells play a central role in the conservation of docosahexaenoic acid by photoreceptor cells after shedding and phagocytosis. *Curr Eye Res*. 1992;11(1):73–83.
13. Kevany BM, Palczewski K. Phagocytosis of retinal rod and cone photoreceptors. *Physiology (Bethesda)*. 2010;25(1):8–15.
14. Strauss O. The retinal pigment epithelium in visual function. *Physiol Rev*. 2005;85(3):845–881.
15. Young RW. Pathophysiology of age-related macular degeneration. *Surv Ophthalmol*. 1987;31(5):291–306.
16. Shamsi FA, Boulton M. Inhibition of RPE lysosomal and antioxidant activity by the age pigment lipofuscin. *Invest Ophthalmol Vis Sci*. 2001;42(12):3041–3046.
17. Kopitz J, Holz FG, Kaemmerer E, et al. Lipids and lipid peroxidation products in the pathogenesis of age-related macular degeneration. *Biochimie*. 2004;86(11):825–831.
18. Ayala A, Munoz MF, Arguelles S. Lipid peroxidation: production, metabolism, and

signaling mechanisms of malondialdehyde and 4-hydroxy-2-nonenal. *Oxid Med Cell Longev*. 2014;2014:360438.
19. Hohn A, Konig J, Grune T. Protein oxidation in aging and the removal of oxidized proteins. *J Proteomics*. 2013;92:132–159.
20. Schutt F, Bergmann M, Holz FG, et al. Proteins modified by malondialdehyde, 4-hydroxynonenal, or advanced glycation end products in lipofuscin of human retinal pigment epithelium. *Invest Ophthalmol Vis Sci*. 2003;44(8):3663–3668.
21. Schutt F, Ueberle B, Schnolzer M, et al. Proteome analysis of lipofuscin in human retinal pigment epithelial cells. *FEBS Lett*. 2002;528(1-3):217–221.
22. Esterbauer H, Schaur RJ, Zollner H. Chemistry and biochemistry of 4-hydroxynonenal, malonaldehyde and related aldehydes. *Free Radic Biol Med*. 1991;11(1):81–128.
23. Kaemmerer E, Schutt F, Krohne TU, et al. Effects of lipid peroxidation-related protein modifications on RPE lysosomal functions and POS phagocytosis. *Invest Ophthalmol Vis Sci*. 2007;48(3):1342–1347.
24. Krohne TU, Kaemmerer E, Holz FG, et al. Lipid peroxidation products reduce lysosomal protease activities in human retinal pigment epithelial cells via two different mechanisms of action. *Exp Eye Res*. 2010;90(2):261–266.
25. Imai H, Arai Z. Hydrolysis of 1,1,3,3-tetramethoxypropane and spectrophotometric determination of its product, malondialdehyde. *Bunseki Kagaku*. 1991;40(3):143–147.
26. Kwon TW, Watts BM. Determination of malonaldehyde by ultraviolet spectrophotometry. *J Food Sci*. 1963;28(6):627–630.
27. Lung CC, Fleisher JH, Meinke G, et al. Immunochemical properties of malondialdehyde-protein adducts. *J Immunol Methods*. 1990;128(1):127–132.
28. Schraermeyer U, Enzmann V, Kohen L, et al. Porcine iris pigment epithelial cells can take up retinal outer segments. *Exp Eye Res*. 1997;65(2):277–287.
29. Dunn KC, Aotaki-Keen AE, Putkey FR, et al. ARPE-19, a human retinal pigment epithelial cell line with differentiated properties. *Exp Eye Res*. 1996;62(2):155–169.
30. Maminishkis A, Chen S, Jalickee S, et al. Confluent monolayers of cultured human fetal retinal pigment epithelium exhibit morphology and physiology of native tissue. *Invest Ophthalmol Vis Sci*. 2006;47(8):3612–3624.
31. Sonoda S, Spee C, Barron E, et al. A protocol for the culture and differentiation of highly polarized human retinal pigment epithelial cells. *Nat Protoc*. 2009;4(5):662–673.
32. Terasaki H, Shirasawa M, Otsuka H, et al. Different effects of thrombin on VEGF secretion, proliferation, and permeability in polarized and non-polarized retinal pigment epithelial cells. *Curr Eye Res*. 2015;40(9):936–945.
33. Ye F, Kaneko H, Nagasaka Y, et al. Plasma-activated medium suppresses choroidal neovascularization in mice: a new therapeutic concept for age-related macular degeneration. *Sci Rep*. 2015;5:7705.
34. Ijima R, Kaneko H, Ye F, et al. Interleukin-18 induces retinal pigment epithelium degeneration in mice. *Invest Ophthalmol Vis Sci*. 2014;55(10):6673–6678.
35. Kaneko H, Dridi S, Tarallo V, et al. DICER1 deficit induces Alu RNA toxicity in age-related macular degeneration. *Nature*. 2011;471(7338):325–330.
36. Liang CM, Tai MC, Chang YH, et al. Glucosamine inhibits epithelial-to-mesenchymal transition and migration of retinal pigment epithelium cells in culture and morphologic changes in a mouse model of proliferative vitreoretinopathy. *Acta Ophthalmol*. 2011;89(6):e505–e514.
37. Shirasawa M, Sonoda S, Terasaki H, et al. TNF-alpha disrupts morphologic and functional barrier properties of polarized retinal pigment epithelium. *Exp Eye Res*. 2013;110:59–69.
38. Komatsu M, Waguri S, Koike M, et al. Homeostatic levels of p62 control cytoplasmic inclusion body formation in autophagy-deficient mice. *Cell*. 2007;131(6):1149–1163.
39. Pankiv S, Clausen TH, Lamark T, et al. p62/SQSTM1 binds directly to Atg8/LC3 to facilitate degradation of ubiquitinated protein aggregates by autophagy. *J Biol Chem*. 2007;282(33):24131–24145.
40. Bjørkøy G, Lamark T, Pankiv S, et al. Monitoring autophagic degradation of p62/SQSTM1. *Methods Enzymol*. 2009;452:181–197.
41. Krohne TU, Stratmann NK, Kopitz J, et al. Effects of lipid peroxidation products on lipofuscinogenesis and autophagy in human retinal pigment epithelial cells. *Exp Eye Res*. 2010;90(3):465–471.
42. Sundelin SP, Terman A. Different effects of chloroquine and hydroxychloroquine on lysosomal function in cultured retinal pigment epithelial cells. *APMIS*. 2002;110(6):481–489.
43. Beatty S, Koh H, Phil M, et al. The role of oxidative stress in the pathogenesis of age-related macular degeneration. *Surv Ophthalmol*. 2000;45(2):115–134.

44. Wihlmark U, Wrigstad A, Roberg K, et al. Formation of lipofuscin in cultured retinal pigment epithelial cells exposed to pre-oxidized photoreceptor outer segments. *APMIS*. 1996;104(4):272–279.
45. Lei L, Tzekov R, Li H, et al. Inhibition or stimulation of autophagy affects early formation of lipofuscin-like autofluorescence in the retinal pigment epithelium cell. *Int J Mol Sci*. 2017;18(4):728.
46. Zhang B, Yin X, Li J, et al. Essential contribution of macrophage Tie2 signal mediated autophagy in laser-induced choroidal neovascularization. *Exp Eye Res*. 2020;193:107972.
47. Chan CM, Huang DY, Sekar P, et al. Reactive oxygen species-dependent mitochondrial dynamics and autophagy confer protective effects in retinal pigment epithelial cells against sodium iodate-induced cell death. *J Biomed Sci*. 2019;26(1):40.
48. Jang KH, Hwang Y, Kim E. PARP1 impedes SIRT1-mediated autophagy during degeneration of the retinal pigment epithelium under oxidative stress. *Mol Cells*. 2020;43(7):632–644.
49. Hsu MY, Hsiao YP, Lin YT, et al. Quercetin alleviates the accumulation of superoxide in sodium iodate-induced retinal autophagy by regulating mitochondrial reactive oxygen species homeostasis through enhanced deacetyl-SOD2 via the Nrf2-PGC-1α-Sirt1 pathway. *Antioxidants (Basel, Switzerland)*. 2021;10(7):1125.
50. Gottlieb RA, Carreira RS. Autophagy in health and disease. 5. Mitophagy as a way of life. *Am J Physiol Cell Physiol*. 2010;299(2):C203–C210.
51. Chen H, Chan DC. Mitochondrial dynamics–fusion, fission, movement, and mitophagy–in neurodegenerative diseases. *Human Mol Genet*. 2009;18(R2):R169–R176.
52. Mitter SK, Song C, Qi X, et al. Dysregulated autophagy in the RPE is associated with increased susceptibility to oxidative stress and AMD. *Autophagy*. 2014;10(11):1989–2005.
53. Kaarniranta K, Sinha D, Blasiak J, et al. Autophagy and heterophagy dysregulation leads to retinal pigment epithelium dysfunction and development of age-related macular degeneration. *Autophagy*. 2013;9(7):973–984.
54. Lerner C, Bitto A, Pulliam D, et al. Reduced mammalian target of rapamycin activity facilitates mitochondrial retrograde signaling and increases life span in normal human fibroblasts. *Aging Cell*. 2013;12(6):966–977.
55. Mandal PK, Blanpain C, Rossi DJ. DNA damage response in adult stem cells: pathways and consequences. *Nat Rev Mol Cell Biol*. 2011;12(3):198–202.
56. Lee AC, Fenster BE, Ito H, et al. Ras proteins induce senescence by altering the intracellular levels of reactive oxygen species. *J Biol Chem*. 1999;274(12):7936–7940.
57. Ito K, Hirao A, Arai F, et al. Reactive oxygen species act through p38 MAPK to limit the lifespan of hematopoietic stem cells. *Nat Med*. 2006;12(4):446–451.
58. Marazita MC, Dugour A, Marquioni-Ramella MD, et al. Oxidative stress-induced premature senescence dysregulates VEGF and CFH expression in retinal pigment epithelial cells: implications for age-related macular degeneration. *Redox Biol*. 2016;7:78–87.
59. Zhuge CC, Xu JY, Zhang J, et al. Fullerenol protects retinal pigment epithelial cells from oxidative stress-induced premature senescence via activating SIRT1. *Invest Ophthalmol Vis Sci*. 2014;55(7):4628–4638.
60. Sreekumar PG, Ishikawa K, Spee C, et al. The mitochondrial-derived peptide humanin protects RPE cells from oxidative stress, senescence, and mitochondrial dysfunction. *Invest Ophthalmol Vis Sci*. 2016;57(3):1238–1253.
61. Supanji, Shimomachi M, Hasan MZ, et al. HtrA1 is induced by oxidative stress and enhances cell senescence through p38 MAPK pathway. *Exp Eye Res*. 2013;112:79–92.